HHS Public Access

Author manuscript

Bone. Author manuscript; available in PMC 2023 January 01.

Published in final edited form as:

Bone. 2022 January ; 154: 116228. doi:10.1016/j.bone.2021.116228.

The combination of aging and chronic kidney disease leads to an exacerbated cortical porosity phenotype

Samantha P. Tippen[1], **Corinne E. Metzger**[1], **Elizabeth A. Swallow**[1], **Spencer A. Sacks**[1], **Joseph M. Wallace**[3], **Matthew R. Allen**[1,2,3,4]

[1]Department of Anatomy, Cell Biology, and Physiology, Indiana University School of Medicine, Indianapolis, IN, USA, 46202.

[2]Department of Medicine/Division of Nephrology, Indiana University School of Medicine, Indianapolis, IN, USA, 46202.

[3]Department of Biomedical Engineering, Indiana University Purdue University of Indianapolis, Indianapolis, IN, 46202.

[4]Roudebush Veterans Administration Medical Center, Indianapolis, IN, USA, 46202.

Abstract

Purpose: Chronic kidney disease (CKD) and aging are each independently associated with higher fracture risk. Although CKD is highly prevalent in the aging population, the interaction between these two conditions with respect to bone structure and mechanics is not well understood. The purpose of this study was to examine cortical porosity and mechanical properties in skeletally mature young and aging mice with CKD.

Methods: CKD was induced by feeding 16-week and 78-week male mice 0.2% adenine (AD) for six weeks followed by two weeks of maintenance on a control diet for a total study duration of eight weeks of CKD; control (CON) animals of each age were fed a standard diet. Serum biochemistries, μCT imaging, and mechanical properties via four-point bending were assessed at the endpoint.

Results: Phosphorus, parathyroid hormone, and blood urea nitrogen were elevated in both ages of AD mice compared to age-matched CON; aging AD mice had PTH and BUN values higher than all other groups. Femoral cortical porosity was more than four-fold higher in aging AD mice compared to young AD mice and more than two-fold higher compared to age-matched controls.

Corresponding Author: Matthew R. Allen, Department of Anatomy, Cell Biology, & Physiology, Indiana University School of Medicine, 635 Barnhill Drive, MS 5045, Indianapolis, IN 46202, Office phone: (317) 274-1283, matallen@iu.edu.

CRediT author statement

Samantha P. Tippen: Conceptualization, Data curation, Visualization, Writing – Original draft preparation, Writing – Reviewing and Editing **Corinne E. Metzger**: Conceptualization, Data curation, Writing – Original draft preparation, Writing – Reviewing and Editing **Elizabeth A. Swallow**: Data curation **Spencer A. Sacks**: Data curation **Joseph M. Wallace**: Writing – Reviewing and Editing **Matthew R. Allen**: Conceptualization, Writing – Original draft preparation, Writing – Reviewing and Editing

SPT designed, performed, and analyzed the experiments. CEM, EAS, and SAS assisted with data collection. SPT, CEM, JMW, and MRA collectively designed studies and interpreted the data. SPT, CEM, and MRA wrote the manuscript.

Structural and estimated material mechanical properties were both lower in aging mice, but there were no significant interactions between AD treatment and age.

Conclusion: These data show an interaction between CKD and aging that produces a more severe biochemical and cortical bone phenotype. This highlights the importance of studying mechanisms and potential interventions in both young and aged animals to translate to a broader spectrum of CKD patients.

Keywords

Bone; parathyroid hormone; cortical porosity; adenine; mechanical properties

1.1 INTRODUCTION

Chronic kidney disease (CKD) and aging are each independently associated with higher risk of fracture. Although ~38% of the U.S. population of 65+ years has CKD[1], the interaction between aging and CKD with respect to bone structure and mechanics is not well understood. Skeletal fragility associated with CKD is primarily due to deterioration of cortical bone and development of holes within the cortical bone (cortical porosity), the region that principally determines the mechanical properties of the bone[2]. Often due to unbalanced remodeling, cortical porosity also occurs in aging, although to a lesser degree than in CKD[3]. Interactions between CKD and aging are important to understand in order to frame efficacy of future treatments for the aging CKD population.

Despite osteonal remodeling not being a normal part of rodent physiology, we previously have shown robust cortical porosity development in rodents with CKD[1–3], indicating the potential for overlapping mechanisms of porosity development in rodents and humans. We have shown that mice with adenine-induced CKD have a skeletal phenotype that includes cortical porosity and thinning[4]. Additionally, we and others have documented age-induced cortical porosity in male mice without impaired renal function[5]. The goal of this study was to compare the individual and combined effects of aging and CKD on cortical porosity and mechanical properties utilizing the adenine-induced CKD model in young, skeletally mature and aging mice. We hypothesized that interactions would exist between CKD and aging for cortical porosity and whole-bone mechanical properties.

1.2 MATERIALS AND METHODS

1.2.1 Animals

Male C57Bl/6J mice were obtained from Jackson Laboratories (JAX stock #000-664, Bar Harbor, ME, USA) at 15- and 77-weeks of age (n=16/age) and group housed at an institutionally approved animal facility with 12h light/dark cycles. After one week of acclimation, all mice were switched to a casein-based diet with adjusted calcium and phosphorus (0.9% P, 0.6% Ca). Half of the mice were given the same casein-based diet with 0.2% adenine (AD; Envigo-Teklad Diets, Madison, WI, USA) to induce CKD while the remaining mice served as age-matched controls (CON; n=8/group). After six weeks on the adenine diet, the AD mice were switched to the casein diet for an additional two weeks to produce an eight-week total timeline. Body weight was measured weekly, and

animals were monitored for health daily. Animals were euthanized via exsanguination under isoflurane anesthesia, and blood was collected from the heart for biochemical analyses. One femur was fixed in 10% neutral buffered formalin, and one tibia was placed in saline-soaked gauze and frozen. All animal procedures were approved by the Indiana University School of Medicine Institutional Animal Care and Use Committee prior to the initiation of experimental protocols, and methods were carried out in accordance with relevant guidelines and regulations.

1.2.2 Serum Biochemistries

Cardiac blood collected at time of termination was used to measure serum calcium and phosphorus (Pointe Scientific, Canton, MI, USA) and blood urea nitrogen (BUN) (BioAssay Systems, Hayward, CA, USA) via colorimetric assays. Serum parathyroid hormone (PTH) was measured via ELISA (Immutopics Quidel, San Diego, CA, USA) as previously described[6].

1.2.3 Ex Vivo Micro-Computed Tomography of the Femur

Distal femora were scanned on a SkyScan 1172 system (Bruker, Billerica, MA, USA) using a custom holder that allows scanning of 3 bones at a time[7] with the following settings: 60kV, medium camera, 0.5 aluminum filter, frame averaging of 2, 0.7 rotation step, and 8μm voxel size. Trabecular bone architecture was analyzed from a 1mm region of interest (ROI) just proximal to the distal growth plate. Measures of trabecular bone included bone volume fraction/total volume, trabecular thickness, trabecular number, and trabecular spacing. Cortical bone geometry was analyzed from five consecutive slices ~2.5mm proximal to the distal growth plate in a region proximal to the trabecular bone of the distal femur. Measures of cortical bone included cortical bone area, cortical thickness, and cortical porosity. Cortical porosity was determined by assessing void area between the periosteal and endosteal surfaces, presented as a percentage of overall cortical bone area. ROIs were hand-drawn with a binary threshold of 100 – 255. All nomenclature followed standard recommendations[8]. A visual interpretation of our analysis process can be found in Supplemental Figure 1.

Tibial midshafts were group-scanned using the SkyScan 1172 system (Bruker, Billerica, MA, USA) with a 0.5 aluminum filter and a 9μm voxel size to assess geometric properties for stress/strain calculations following mechanical testing. Cortical bone geometry was analyzed from five consecutive slices selected at the location of the proximal tibiofibular joint (TFJ); measures of cortical bone included cortical bone area, cortical thickness, and cortical porosity.

1.2.4 Four-Point Bending of the Tibia

Tibiae underwent four-point bending (TA Instruments, New Castle, DE, USA) as previously described[5]. Briefly, bones were thawed to room temperature soaked in PBS. The anterior surface was placed on two metal supports located ±9mm from the mid-diaphysis testing site, and the upper supports were centered on the bone with a span of ±4mm. Specimens were loaded to failure at a rate of 0.025mm/sec, producing a force-displacement curve for each sample. Structural mechanical properties (yield/ultimate load, stiffness, pre-yield/post-yield/

total displacement, and pre-yield/post-yield/total energy to failure) were obtained directly from the curves using a MATLAB code, while estimated material properties (ultimate stress, elastic modulus, strain, resilience, total toughness) were derived from force-displacement curves and geometric properties noted above using standard beam-bending equations for four-point bending.

1.2.5 Statistical Analyses

Statistical analyses were completed in SPSS Statistics 25 (IBM, Armonk, NY, USA). Data were analyzed as a 2×2 factorial ANOVA (age-by-disease) with main effects of disease (CKD versus control), age (young versus aging), and disease-by-age interactions noted. When the 2×2 ANOVA was statistically significant ($p<0.05$), an all-groups Duncan post-hoc analysis was applied to determine individual group differences. Linear regressions were performed to assess the relationships between cortical porosity, PTH, and select mechanical properties. All data are presented as mean ± standard deviation.

1.3 RESULTS

Due to low body condition scoring, one young adenine-fed mouse was euthanized at week 5, and one aging adenine-fed mouse was euthanized at week 7. Two aging adenine-fed mice died of unknown causes at week 1 and week 7; one aging control mouse died of unknown causes prior to the start of the study. This resulted in group sizes of young control (n=8), young adenine (n=7), aging control (n=7), and aging adenine (n=5).

1.3.1 Ingestion of adenine resulted in reduced food intake and body weight in both ages.

There was an age-by-disease interaction for endpoint body weight ($p<0.0001$). Both young (−37%) and aging (−29%) AD mice had significantly lower values than their age-matched controls (Figure 1B). Body weight differences were consistent with altered food intake. While on the adenine diet, young mice consumed 54% and aging mice consumed 55% of the total food consumed by age-matched mice on the control diet; with resumption of the control diet at week 7, food intake increased in both young (+62%) and aging (+67%) mice.

1.3.2 Biochemical indices were influenced by both age and disease.

Although there was no age-by-disease interaction for serum phosphorus, both young (+40%) and aging (+44%) AD mice had significantly higher values than their age-matched controls (Figure 1C). There were no differences in serum calcium across the four groups (Figure 1D). There was an age-by-disease interaction for serum BUN ($p<0.0001$) and serum PTH ($p<0.0001$). While there was no difference between young and aging CON mice, both young (+59%) and aging (+67%) AD mice had significantly higher values than their age-matched controls. Aging AD mice had BUN levels significantly higher than young AD animals (+33%) (Figure 1E). Young and aging control mice had no differences in PTH. Aging AD mice had PTH levels that were nine-fold higher than their age-matched controls ($p<0.05$). The young AD group had four-fold higher PTH than the young CON group, but this did not reach statistical significance (Figure 1F).

1.3.3 Cortical bone structure was compromised by both age and disease.

There was an age-by-disease interaction for femoral cortical porosity (p=0.001). Aging AD mice had +78% higher femoral porosity than young AD mice and +63% higher femoral porosity than age-matched controls (Figure 2A). The young AD group exhibited three-fold higher femoral porosity than the young CON group (p<0.0001). From linear regression analysis, PTH levels predicted ~35% of femoral cortical porosity across this dataset. Although there were effects of age (p=0.014) and disease (p=0.004) on tibial midshaft cortical porosity, the age-by-disease interaction did not reach significance (p=0.051). Aging AD mice had +76% higher tibial cortical porosity than young AD mice and +86% higher tibial cortical porosity than age-matched counterparts (Figure 2B).

Femoral cortical bone area was affected by diet (p<0.0001), with aging AD mice having −36% lower cortical area and young AD mice having −32% lower cortical area compared to age-matched counterparts (Figure 2C). Both age (p<0.0001) and disease (p<0.0001) affected femoral cortical thickness; both young and aging AD mice had roughly 30–38% lower femoral cortical thickness compared to age-matched counterparts (Figure 2E). Although there were not differences due to age, both young and aging AD mice had 45–55% lower tibial cortical area and 45–60% lower tibial cortical thickness compared to age-matched counterparts (Figures 2D and 2F). There were no differences in distal femur trabecular bone volume across groups but interaction effects existed for both trabecular thickness (p=0.019) and trabecular separation (p<0.0001) (Table 1).

1.3.4 Mechanical properties were negatively affected by both age and disease.

There were no age-by-disease interactions across mechanical properties but several properties had independent age and disease effects. Structural properties of ultimate force, stiffness, and total work and estimated material properties of ultimate stress, resilience, and toughness were all significantly lower in adenine-fed mice compared to controls (Table 1). Structural properties of ultimate force, total displacement, and total work and estimated material properties of ultimate stress, modulus, resilience, and toughness were all significantly lower in aging mice compared to young mice (Table 1). To assess whether periosteal expansion occurred, total bone area and periosteal perimeter were measured. There were no differences in total bone area (all bone and marrow tissue; p=0.095) or periosteal perimeter (p=0.457). From linear regression models, tibial cortical porosity levels predicted 22% and 15% of the variability in ultimate force and toughness, respectively.

1.4 DISCUSSION

The primary finding of this study is that while both young and aging male C57Bl/6J mice are negatively impacted by adenine-induced CKD, aging mice exhibit a more severe phenotype with greater cortical porosity and higher PTH than young mice. Adenine-induced CKD in both ages led to reduced structural and estimated material mechanical properties with no significant interactions between the two conditions (age and disease).

There are multiple animal models that allow researchers to study CKD, two of the most common being 5/6-nephrectomy and oral ingestion of adenine. Surgical methods have

several key limitations, including post-surgical mortality, variability in surgical technique, and rapid onset of kidney function decline[9]. Adenine was first utilized in a rat model where higher doses (0.75% adenine) caused rapid, severe kidney alterations that were more consistent with nephrotoxic disease; however, reductions in dosage to 0.25% adenine produced a milder and more gradual disease more consistent with CKD[10]. Studies from our lab using a casein-based adenine diet for mice have used a 0.2% dose and shown it produces progressive loss of kidney function and recapitulates the biochemical and skeletal effects seen in CKD-MBD[9]. One limitation of the adenine diet is weight loss due to reduced food intake, which could contribute to some, but unlikely all, of the skeletal changes in the model. To our knowledge, the adenine diet has not been utilized to study aging mice, which is a key strength and novelty of the current paper.

It is well-established that cortical porosity increases with age[11,12]. Burghardt et. al (2010) found that cortical porosity was more strongly associated with age compared to other cortical metrics, such as cortical thickness and cortical bone area[13]. Analyses of human iliac crest biopsies have documented that higher cortical porosity with age is more often due to an increase in the size of individual pores rather than areal pore density; additionally, porosity was tied to remodeling of existing canals rather than the generation of new canals[14]. Despite known differences between human and rodent cortical bone structure and physiology, mice develop a skeletal aging phenotype that includes age-related cortical porosity[15]. In this current study, untreated aging mice had lower cortical thickness and cortical area as well as ~6% higher femoral cortical porosity, demonstrating age-induced cortical bone alterations. Although intracortical osteonal remodeling is not part of normal rodent bone physiology, rodents with CKD still develop cortical porosity like humans. We hypothesize there are overlapping mechanisms driving pore development in both species, likely driven through the initiation of resorption by osteoclasts from the endocortical surface that then tunnel through the cortical bone.

In humans and rodents, high circulating PTH is associated with loss of cortical bone and cortical porosity development[2,6,16]. With patients that have declining renal function, serum PTH can be dysregulated and rise uncontrollably[17]. In this current study, our results are consistent with previous studies that demonstrate that adenine-induced CKD results in elevated PTH[4,6,18]. Importantly, our study shows that aging mice fed adenine had elevations in PTH that were notably higher compared to young AD, specifically 72% higher than young AD mice. The mechanisms leading to more robust PTH response to CKD in aging mice is not known, but it indicates that alterations caused by impaired renal function may be exacerbated by age.

While age-related cortical porosity occurs slowly, CKD-induced cortical porosity in both rodents and humans changes rapidly over time[2,19]. Evaluation of CKD patients demonstrates 4–5% loss of cortical bone density per year[20], illustrating that CKD more rapidly and significantly affects the cortical bone than aging. CKD produces robust cortical porosity, even in younger rodents[4,6], but how this impacts porosity in aging animals is less understood. In the present study, aging AD mice had 78% higher femoral cortical porosity than young AD mice and 63% higher femoral porosity than age-matched counterparts. Previously, Heveran et. al (2019) examined young (12-week) and old (84-week) mice with

5/6 nephrectomy and found that the reduced bone material quality in CKD was distinct from age-related bone quality changes, but no differences in cortical porosity were observed[21]. In our study, adenine-induced CKD caused 4.2-fold higher PTH in young mice and 9-fold higher PTH in aging vs. age-matched counterparts, while the 5/6 nephrectomy in Heveran et. al caused ~2-fold higher PTH across both ages[21]. Since high PTH is associated with cortical porosity in CKD, we hypothesize this difference, namely the higher PTH induced by the adenine model, was largely responsible for the adenine-induced cortical porosity and the heightened porosity development in the aging mice. Unlike our previous study[6], this study did not measure PTH across the experimental timeline, so we can only speculate that the elevated cortical porosity in adenine mice was mediated largely by elevated PTH levels. This result reiterates the importance of PTH in cortical porosity development and certainly supports the clinical approach of controlling PTH levels in CKD patients.

Along with increases in cortical porosity, adenine-induced CKD also resulted in lower cortical thickness and cortical bone area, but no differences between young and aging mice were observed. Because cortical bone is closely linked to the mechanical strength of bone, deterioration of cortical bone, through porosity and cortical thinning, is associated with a decline in mechanical properties. Previously, we demonstrated adenine-induced CKD in male mice reduced structural properties, including ultimate force and stiffness, while estimated material properties, such as toughness, showed no differences between CON and AD[4]. In the current study, there were independent effects of age and disease on both structural and material properties, although no interaction effects were observed. Interestingly, the aging AD mice even with higher cortical porosity did not have greater alterations in mechanical properties vs. the young AD mice. These findings allude to a potential compensatory mechanism that may occur within aging bone to preserve bone mechanical properties despite increasing cortical porosity. Analysis of total bone area and periosteal perimeter of tibiae tested showed no differences across groups, indicating that periosteal expansion is not a likely compensatory mechanism in this model.

Limitations of the current study include the use of only male mice. We chose to utilize male mice, because we previously showed that with aging, male mice exhibit higher PTH and cortical porosity than aging, female mice without kidney disease[5]. However, this prior study found sex-based differences in regulation of phosphate metabolism in young and aging mice[5], so future studies should assess whether sex-based differences would also be observed in aging mice with CKD. As our focus was on the skeletal manifestations, we used BUN to assess the presence/absence of altered kidney function. We acknowledge that measures, such as GFR or creatinine, can be more specific, and therefore our study is limited in its ability to determine the extent of kidney function or if interactions between aging and CKD occurred with respect to kidney function. The adenine-induced CKD model in mice does cause reduced food intake, which may cause protein malnourishment and lead to metabolic acidosis[22,23]. How each of these components contributes to disease progression and the skeletal phenotype is not addressed by this work. Finally, our study utilized a relatively small sample size for mechanics, which could have affected our ability to find significant interaction effects.

In conclusion, these data demonstrate that combining aging and CKD leads to an exacerbated cortical porosity phenotype that appears linked to the differential elevations of PTH. This highlights the importance of assessing mechanisms and potential interventions in both young and aged animals to translate to a broader spectrum of CKD patients.

Supplementary Material

Refer to Web version on PubMed Central for supplementary material.

Acknowledgements

The authors would like to acknowledge NIH grant T32-AR065971 (SPT). The content is solely the responsibility of the authors and does not necessarily represent the official views of the NIH or IUSM.

REFERENCES

[1]. CDC, Chronic Kidney Disease in the United States, (2019). cdc.gov/kidneydisease/publications-resources/2019-national-facts.html (accessed April 5, 2020).

[2]. Nickolas TL, Stein EM, Dworakowski E, Nishiyama KK, Komandah-Kosseh M, Zhang CA, McMahon DJ, Liu XS, Boutroy S, Cremers S, Shane E, Rapid cortical bone loss in patients with chronic kidney disease, Journal of Bone and Mineral Research. 28 (2013) 1811–1820. 10.1002/jbmr.1916. [PubMed: 23456850]

[3]. Bala Y, Zebaze R, Ghasem-Zadeh A, Atkinson EJ, Iuliano S, Peterson JM, Amin S, Bjørnerem Å, Melton LJ, Johansson H, Kanis JA, Khosla S, Seeman E, Cortical porosity identifies women with osteopenia at increased risk for forearm fractures, Journal of Bone and Mineral Research. 29 (2014) 1356–1362. 10.1002/jbmr.2167. [PubMed: 24519558]

[4]. Metzger CE, Swallow EA, Stacy AJ, Allen MR, Adenine-induced chronic kidney disease induces a similar skeletal phenotype in male and female C57BL/6 mice with more severe deficits in cortical bone properties of male mice, PLoS ONE. 16 (2021). 10.1371/journal.pone.0250438.

[5]. Tippen SP, Noonan ML, Ni P, Metzger CE, Swallow EA, Sacks SA, Chen NX, Thompson WR, Prideaux M, Atkins GJ, Moe SM, Allen MR, White KE, Age and sex effects on FGF23-mediated response to mild phosphate challenge, Bone. 146 (2021). 10.1016/j.bone.2021.115885.

[6]. Metzger CE, Swallow EA, Allen MR, Elevations in Cortical Porosity Occur Prior to Significant Rise in Serum Parathyroid Hormone in Young Female Mice with Adenine-Induced CKD, Calcified Tissue International. 106 (2020) 392–400. 10.1007/s00223-019-00642-w. [PubMed: 31832725]

[7]. Kohler R, Tastad CA, Stacy AJ, Swallow EA, Metzger CE, Allen MR, Wallace JM, The Effect of Single Versus Group μCT on the Detection of Trabecular and Cortical Disease Phenotypes in Mouse Bones, JBMR Plus. (2021) e10473. 10.1002/jbm4.10473. [PubMed: 33869991]

[8]. Bouxsein ML, Boyd SK, Christiansen BA, Guldberg RE, Jepsen KJ, Müller R, Guidelines for assessment of bone microstructure in rodents using micro-computed tomography, Journal of Bone and Mineral Research. 25 (2010) 1468–1486. 10.1002/jbmr.141. [PubMed: 20533309]

[9]. Jia T, Olauson H, Lindberg K, Amin R, Edvardsson K, Lindholm B, Andersson G, Wernerson A, Sabbagh Y, Schiavi S, Larsson T, A novel model of adenine-induced tubulointerstitial nephropathy in mice, BMC Nephrology. 14 (2013). 10.1186/1471-2369-14-116.

[10]. Diwan V, Brown L, Gobe G, Adenine-induced chronic kidney disease in rats, Nephrology (Carlton, Vic.). 23 (2018) 5–11. 10.1111/NEP.13180.

[11]. Atkinson PJ, Changes in resorption spaces in femoral cortical bone with age, The Journal of Pathology and Bacteriology. 89 (1965) 173–178. 10.1002/path.1700890118. [PubMed: 14263459]

[12]. Jowsey J, Age changes in human bone, Clinical Orthopaedics and Related Research. 17 (1960) 210–217.

[13]. Burghardt AJ, Kazakia GJ, Ramachandran S, Link TM, Majumdar S, Age- and gender-related differences in the geometric properties and biomechanical significance of intracortical porosity in the distal radius and tibia, Journal of Bone and Mineral Research. 25 (2010) 983–993. 10.1359/jbmr.091104. [PubMed: 19888900]

[14]. Andreasen CM, Delaisse JM, van der Eerden BCJ, van Leeuwen JPTM, Ding M, Andersen TL, Understanding Age-Induced Cortical Porosity in Women: The Accumulation and Coalescence of Eroded Cavities Upon Existing Intracortical Canals Is the Main Contributor, Journal of Bone and Mineral Research. 33 (2018) 606–620. 10.1002/jbmr.3354. [PubMed: 29193312]

[15]. Jilka RL, Almeida M, Ambrogini E, Han L, Roberson PK, Weinstein RS, Manolagas SC, Decreased oxidative stress and greater bone anabolism in the aged, when compared to the young, murine skeleton with parathyroid hormone administration, Aging Cell. 9 (2010) 851–867. 10.1111/j.1474-9726.2010.00616.x. [PubMed: 20698835]

[16]. Newman CL, Moe SM, Chen NX, Hammond MA, Wallace JM, Nyman JS, Allen MR, Cortical bone mechanical properties are altered in an animal model of progressive chronic kidney disease, PLoS ONE. 9 (2014). 10.1371/journal.pone.0099262.

[17]. Niculescu DA, Deacu LG, Caragheorgheopol A, Popescu N, Ghemigian A, Procopiuc C, Rosca R, Poiana C, Combined Effects of Vitamin D Status, Renal Function and Age on Serum Parathyroid Hormone Levels, Frontiers in Endocrinology. 12 (2021) 1. 10.3389/fendo.2021.657991.

[18]. Metzger CE, Swallow EA, Stacy AJ, Tippen SP, Hammond MA, Chen NX, Moe SM, Allen MR, Reversing cortical porosity: Cortical pore infilling in preclinical models of chronic kidney disease, Bone. 143 (2021). 10.1016/j.bone.2020.115632.

[19]. McNerny EMB, Buening DT, Aref MW, Chen NX, Moe SM, Allen MR, Time course of rapid bone loss and cortical porosity formation observed by longitudinal μCT in a rat model of CKD, Bone. 125 (2019) 16–24. 10.1016/j.bone.2019.05.002. [PubMed: 31059864]

[20]. Costa LR, Carvalho AB, Bittencourt AL, Rochitte CE, Canziani MEF, Cortical unlike trabecular bone loss is not associated with vascular calcification progression in CKD patients, BMC Nephrology. 21 (2020) 1–7. 10.1186/s12882-020-01756-2.

[21]. Heveran CM, Schurman CA, Acevedo C, Livingston EW, Howe D, Schaible EG, Hunt HB, Rauff A, Donnelly E, Carpenter RD, Levi M, Lau AG, Bateman TA, Alliston T, King KB, Ferguson VL, Chronic kidney disease and aging differentially diminish bone material and microarchitecture in C57Bl/6 mice, Bone. 127 (2019) 91–103. 10.1016/j.bone.2019.04.019. [PubMed: 31055118]

[22]. Zha Y, Qian Q, Protein Nutrition and Malnutrition in CKD and ESRD, Nutrients. 9 (2017). 10.3390/NU9030208.

[23]. Laboux T, Azar R, Dietary control of metabolic acidosis in chronic kidney disease, Nephrologie & Therapeutique. 15 (2019) 491–497. 10.1016/J.NEPHRO.2018.12.001. [PubMed: 31056406]

Highlights

- Adenine-induced CKD causes high PTH and cortical porosity in young and aging mice.
- Aging adenine mice had greater PTH and cortical porosity than young adenine mice.
- Adenine and aging both independently impacted bone mechanics.

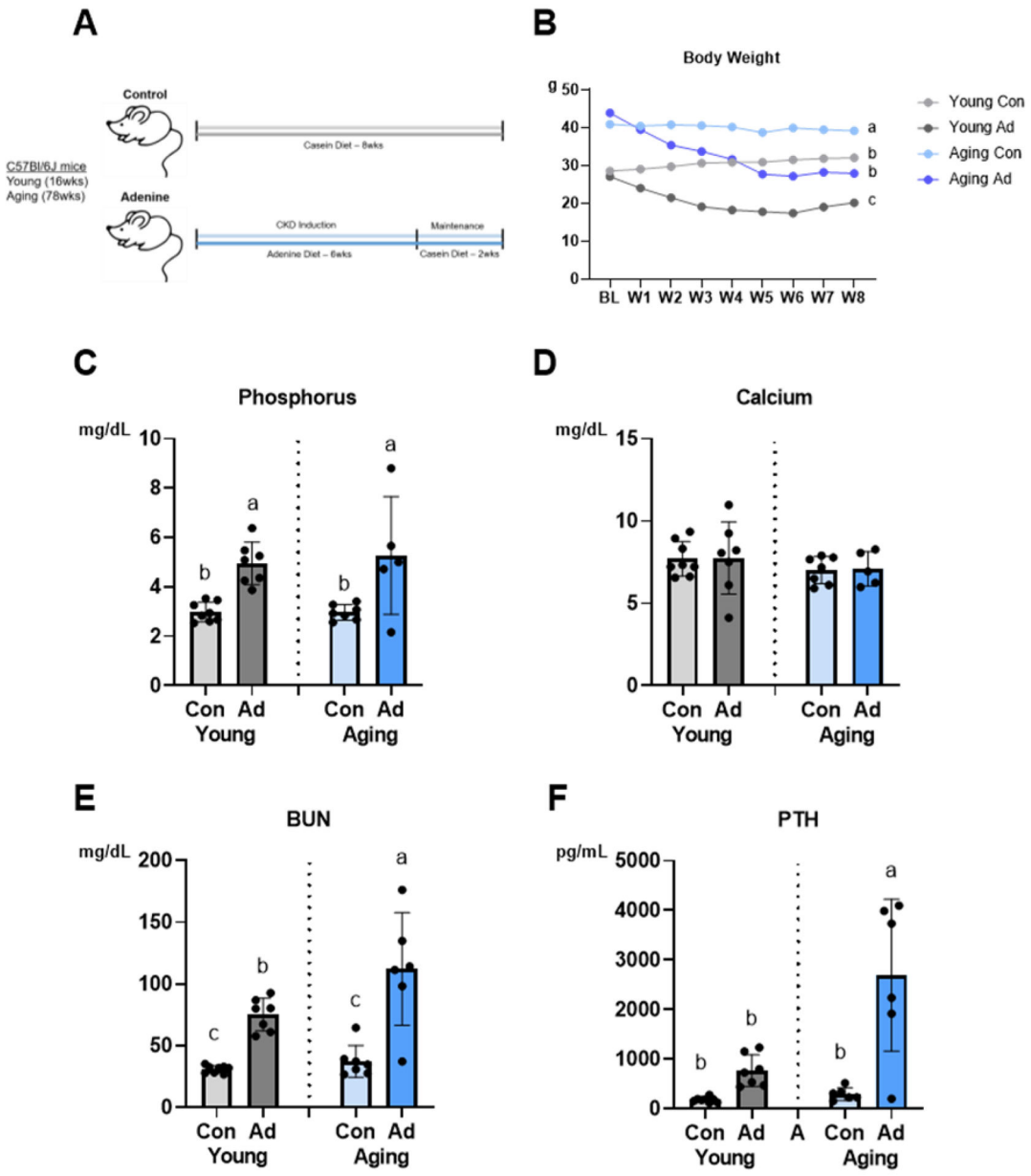

Figure 1:

Biochemical parameters reveal interactions between aging and CKD. **A** Schematic of study design (n=6–8 per group). **B** Both adenine-fed groups (AD) had lower endpoint body weight ($p<0.0001$) compared to control (Con) with an effect of age ($p=0.002$) and an age-by-disease interaction ($p<0.0001$). **C** Serum phosphorus was highest in adenine-fed groups ($p<0.0001$), although there was no age-by-disease interaction effect. **D** There were no differences in serum calcium across groups. **E** Blood urea nitrogen (BUN) was highest in aging AD mice ($p=0.02$) with an effect of disease ($p<0.0001$) and an age-by-disease interaction ($p<0.0001$). **F** Parathyroid hormone (PTH) was highest in aging AD mice ($p=0.002$) with an effect of disease ($p<0.0001$) and an interaction effect ($p<0.0001$). Data are presented as mean ±

standard deviation. Bars with different letter notations are statistically different from each other ($p<0.05$).

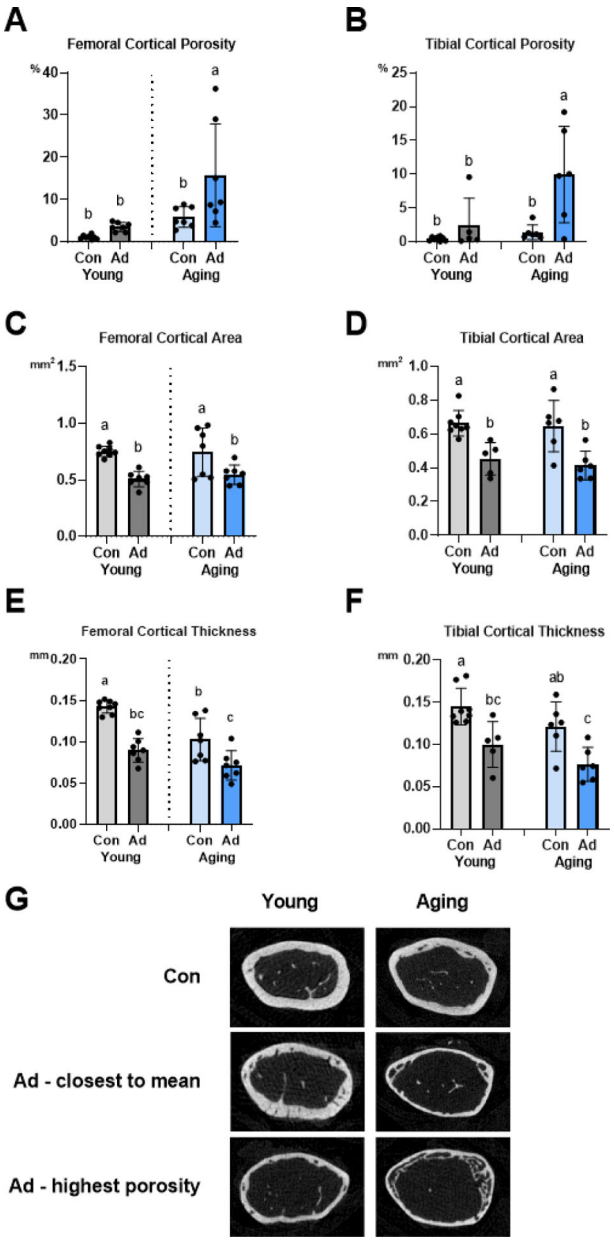

Figure 2:

Cortical bone parameters in femur and tibia are compromised with aging and CKD. **A** Femoral cortical porosity was highest in aging AD mice (p=0.001) with an effect of disease (p=0.012) and an interaction effect (p=0.001). **B** Tibial cortical porosity was also highest in aging AD mice (p=0.014) with an effect of diet (p=0.004) but no interaction effect. **C** Regardless of age, AD mice had the lowest femoral cortical bone area (p<0.0001) without an age-by-disease interaction effect. **D** Regardless of age, CON mice had the highest tibial cortical bone area (p<0.0001) without an age-by-disease interaction. **E** Adenine-fed groups exhibited the lower femoral cortical thickness (p<0.0001) with an effect of age (p<0.0001) but no age-by-disease interaction. **F** Tibial cortical thickness was highest in young CON mice (p=0.026) with an effect of disease (p<0.0001) but no interaction effect.

G Representative μCT images of the femur (CON, AD closest to mean for porosity, and AD highest porosity) for young and aging mice. Data are presented as mean ± standard deviation. Bars with different letter notations are statistically different from each other ($p<0.05$).

Table 1.

Trabecular bone architecture and cortical bone mechanical properties.

	Young – Con	Young – Ad	Aging – Con	Aging - Ad	Disease p-value	Age p-value	Disease x Age p-value
Trabecular bone volume/ tissue volume (%)	6.3±1.1	5.1±1.7	5.4±1.9	4.6±1.9	0.299	0.130	0.706
Trabecular thickness (mm)	0.04±0.01^{ab}	0.05±0.01^{b}	0.04±0.003^{a}	0.04±0.003^{ab}	**0.024**	**0.018**	**0.019**
Trabecular spacing (mm)	0.25±0.02^{b}	0.33±0.04^{b}	0.27±0.03^{a}	0.34±0.06^{a}	0.231	**<0.0001**	**<0.0001**
Trabecular number (1/mm)	1.49±0.28	1.10±0.43	1.45±0.44	1.09±0.45	0.882	**0.018**	0.936
Ultimate Force (N)	14.7±1.6^{a}	8.3±1.0^{bc}	10.3±4.0^{b}	5.6±2.0^{c}	**<0.0001**	**0.003**	0.395
Total Displacement (μm)	917±387^{a}	1075±467^{a}	463±172^{b}	455±211^{b}	0.582	**0.001**	0.544
Stiffness (N/mm)	82.57±16.83^{a}	40.91±15.44^{b}	68.73±20.71^{a}	36.45±9.44^{b}	**<0.0001**	0.195	0.5
Total Work (mJ)	8.08±2.62^{a}	5.45±3.15^{ab}	3.34±2.01^{bc}	1.48±1.14^{c}	**0.03**	**<0.0001**	0.696
Ultimate Stress (MPa)	167±53^{a}	90±22^{b}	98±27^{b}	66±24^{b}	**0.002**	**0.005**	0.153
Modulus (GPa)	11.0±3.8^{a}	4.6±2.1^{b}	7.2±2.2^{b}	4.5±1.2^{b}	0.089	**<0.0001**	0.107
Resilience (MPa)	1.04±0.57^{a}	0.41±0.32^{b}	0.51±0.25^{b}	0.14±0.05^{b}	**0.004**	**0.018**	0.406
Toughness (MPa)	7.37±2.12^{a}	5.38±2.20^{a}	2.94±1.51^{b}	1.69±1.41^{b}	**0.045**	**<0.0001**	0.632

Data provided as mean ± standard deviation. Groups with different letter notations are statistically different from each other ($p<0.05$).